

## Specific heat of clustered low dimensional magnetic systems

This article has been downloaded from IOPscience. Please scroll down to see the full text article.

2007 J. Phys.: Condens. Matter 19 446203

(<http://iopscience.iop.org/0953-8984/19/44/446203>)

View [the table of contents for this issue](#), or go to the [journal homepage](#) for more

Download details:

IP Address: 129.252.86.83

The article was downloaded on 29/05/2010 at 06:30

Please note that [terms and conditions apply](#).

## Specific heat of clustered low dimensional magnetic systems

M S Reis<sup>1</sup>, A Moreira dos Santos<sup>1</sup>, V S Amaral<sup>1</sup>, A M Souza<sup>2</sup>, P Brandão<sup>3</sup>,  
J Rocha<sup>3</sup>, N Tristan<sup>4</sup>, R Klingeler<sup>4</sup>, B Büchner<sup>4</sup>, O Volkova<sup>5</sup> and  
A N Vasiliev<sup>5</sup>

<sup>1</sup> Physics Department and CICECO, Universidade de Aveiro, 3810-193 Aveiro, Portugal

<sup>2</sup> Centro Brasileiro de Pesquisas Físicas, Rua Dr Xavier Sigaud 150, Urca,  
Rio de Janeiro-RJ22290-180, Brazil

<sup>3</sup> Chemistry Department and CICECO, Universidade de Aveiro, 3810-193 Aveiro, Portugal

<sup>4</sup> Leibniz Institute of Solid State and Materials Research (IFW) Dresden, 01069 Dresden, Germany

<sup>5</sup> Moscow State University, 119992 Moscow, Russia

E-mail: [marior@fis.ua.pt](mailto:marior@fis.ua.pt) (M S Reis)

Received 28 March 2007, in final form 27 September 2007

Published 16 October 2007

Online at [stacks.iop.org/JPhysCM/19/446203](http://stacks.iop.org/JPhysCM/19/446203)

### Abstract

Homometallic ferrimagnetism is quite difficult to find in Nature, and this fact makes  $\text{Na}_2\text{Cu}_5\text{Si}_4\text{O}_{14}$  an interesting material due to its ferrimagnetic arrangement of Cu ions in a zigzag chain with dimers and trimers. In view of this, we developed a theoretical model for the magnetic specific heat of a homometallic ferrimagnet and then compared it with experimental data for  $\text{Na}_2\text{Cu}_5\text{Si}_4\text{O}_{14}$  compound. The successful comparison validates the model and further analysis makes it possible to predict anomalous behavior of this low dimensional magnetic system, due to the crossing of the energy levels.

### 1. Introduction

Low dimensional quantum magnetism is an emerging field that has been attracting much attention in recent years. Magnetic chain systems in particular have been studied in detail because of their diversity, namely with respect to (i) the type of the magnetic interaction, antiferromagnetic [1] or ferromagnetic [2], (ii) the different magnetic elements—homometallic [3] or heterometallic [4]—and (iii) the topology of the magnetic centers, i.e. the spatial arrangement of the different magnetic exchange terms such as spin ladders [5] and ferris wheels [6]. This variety of phenomena results in the occurrence of a wealth of physical phenomena where notable examples are Haldane chains [7–9], and spin–Peierls transitions [10].

From the experimental point of view, while the understanding of the magnetic susceptibility behavior is rather straightforward, the analysis of other thermodynamical properties, such as the magnetic specific heat, is rather non-trivial, since this quantity is always compounded

with other degrees of freedom, such as lattice and electronic contributions. Ways to avoid this problem are threefold: (i) subtraction of theoretical electronic and lattice terms [11], (ii) chemical synthesis, when possible, of a non-magnetic analog of the compound, to extract the contributions to the specific heat [12] or (iii) measurement under several values of magnetic fields, to obtain information related specifically to the magnetic part of the specific heat [13]. Furthermore, unlike what is observed in three-dimensional systems (where a well defined magnetic transition is observed), in low dimensional systems the magnetic contribution to the total specific heat is small, when compared to the lattice term, and is often spread out over a wide temperature range [14]. In fact, to complicate matters further, in most inorganic low dimensional systems, there is a transition to a 3D magnetic ordering at some finite temperature that also contributes to the total specific heat.

Despite these drawbacks, theoretical and experimental studies on the thermodynamical properties of magnetic chains have shown that a wide variety of interesting behaviors can be observed. Particularly interesting are ferrimagnetic chain systems, where the coexistence of ferromagnetic (gapless) and antiferromagnetic (gapped) excitations causes the temperature dependence of the specific heat to display both ferromagnetic and antiferromagnetic aspects [15]. More recently it was shown that ferrimagnetic systems can exhibit an intrinsic (not field induced) double-peak feature in the specific heat [16] and that feature is not exclusive to mixed spin systems, but can be observed in homometallic ferrimagnets. In fact, other results show the occurrence of such a double peak even for ferromagnetic mixed spin chains [17, 18].

Since antiferromagnetic coupling is more prevalent in most compounds than ferromagnetic coupling, ferrimagnetism is a convenient way of obtaining remanent magnetization in an antiferromagnetic system. Ferrimagnetic chain systems, for instance, are obtained through the alternation of magnetic species with different spins with antiferromagnetic interaction, resulting in uncompensated spins. On the other hand, homometallic ferrimagnetism is much less frequent, but can also be observed, usually involving an alternation of the  $g$ -factor as observed for  $\text{Co}_2\text{-EDTA}$  [3], or a topology including odd numbers of metal centers with complex magnetic exchange interactions, as observed for  $(\text{Ca, Sr})_3\text{Cu}_3(\text{PO}_4)_4$  [19] and  $\text{Na}_2\text{Cu}_5\text{Si}_4\text{O}_{14}$  [20].

Recently, we have reported a linear chain copper silicate where ferrimagnetism is observed due to the clustering of odd (trimers) and even (dimers) copper ions along the chain, resulting in ferrimagnetic behavior. We have developed a simplified magnetic Hamiltonian that accounts for the observed magnetic properties of this chain system<sup>6</sup>. This result prompted us to study the thermodynamical character of this chain compound. In the present work we investigate in detail the specific heat properties of such a Hamiltonian; from a theoretical point of view and comparing it with our experimental data.

### 1.1. Structure and magnetic susceptibility

Details on the crystal structure of the copper silicate  $\text{Na}_2\text{Cu}_5\text{Si}_4\text{O}_{14}$  were published elsewhere, as well as the synthesis procedure [21]. It contains a zigzag copper chain with alternating dimers and trimers as shown in figure 1. All the copper ions are in square planar coordination and the dimer and trimer units consist on two and three edge sharing  $\text{CuO}_4$  units, respectively. The magnetic properties of such system have been explained based on a set of three magnetic

<sup>6</sup> In order to obtain a fundamental understanding of molecular magnets, especially those lacking three-dimensional order, many important advances have been made in recent years; not only in the fundamental approaches to solving the magnetic Hamiltonian in an analytical way, as presented in this work, but also others that harness the computational power now readily available. These latter apply powerful techniques based on numerical methods, some of them already reaching the development stage of end-user interfaces (see e.g. the ALPS project—<http://alps.comp-phys.org>).

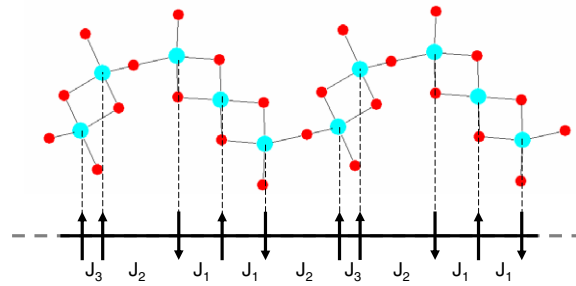


**Figure 1.** Copper chain topology in  $\text{Na}_2\text{Cu}_5\text{Si}_4\text{O}_{14}$ . All copper ions are in square planar coordination (Cu—light, O—dark) (top). The magnetic sequence of the chain (see the text) and its connection with the crystal structure are also shown (bottom).

(This figure is in colour only in the electronic version)

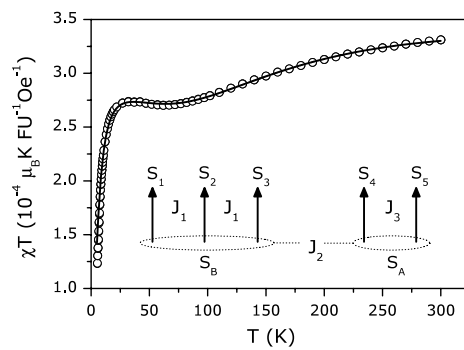


**Figure 2.** Experimental (open circle) and theoretical (full line—see section 1.2 and [20] for details), magnetic susceptibility. The inset represents the ground state arrangement obtained from that fit to the data.

exchange interactions: intratrimer ( $J_1$ ), intradimer ( $J_3$ ), and interdimer–trimer ( $J_2$ ). These chains are separated by  $\text{Si}_2\text{O}_7$  double tetrahedra and are magnetic isolated down to 8 K, where a transition to a 3D antiferromagnetic phase is observed. The arrows in figure 1 represent the ground state arrangement (ferrimagnetic).

The magnetic susceptibility  $\chi T$  versus temperature is shown in figure 2. The plot shows a broad minimum at 64 K, increasing to a maximum at 36 K before a sharp decrease to the ground state. These features have been reported in the literature for one-dimensional compounds, where this broad minimum is associated with 1D ferrimagnetism. The sharp decrease in the plot at low temperatures is shown to be associated with the  $S = 1/2$  ground state of this chain [20].

### 1.2. Magnetic Hamiltonian

In our previous work [20], we have proposed the following Hamiltonian, written in accordance with the inset of figure 2 (general arrangement):

$$\mathcal{H} = -J_1(S_1S_2 + S_2S_3) - J_2S_AS_B - J_3S_4S_5 - g\mu_BHS. \quad (1)$$

All possible states allowed by the system in the basis  $|s, s_A, s_B, s_{B'}\rangle$  are

$$\Omega = \begin{cases} 1 : |5/2, 1, 3/2, 1\rangle \\ 2 : |3/2, 1, 3/2, 1\rangle \\ 3 : |3/2, 1, 1/2, 1\rangle \\ 4 : |3/2, 1, 1/2, 0\rangle \\ 5 : |3/2, 0, 3/2, 1\rangle \\ 6 : |1/2, 0, 1/2, 1\rangle \\ 7 : |1/2, 0, 1/2, 0\rangle \\ 8 : |1/2, 1, 3/2, 1\rangle \\ 9 : |1/2, 1, 1/2, 1\rangle \\ 10 : |1/2, 1, 1/2, 0\rangle \end{cases} \quad (2)$$

and the corresponding zero-field eigenvalues of energy  $E_{\Omega}^{(0)} = E_{\Omega}(H = 0)$  are

$$E_{\Omega}^{(0)} = -\frac{1}{2} \begin{pmatrix} 7/4 & 3 & 2 \\ 7/4 & -2 & 2 \\ -5/4 & 1 & 2 \\ 3/4 & 1 & 2 \\ 7/4 & 0 & 0 \\ -5/4 & 0 & 0 \\ 3/4 & 0 & 0 \\ 7/4 & -5 & 2 \\ -5/4 & -2 & 2 \\ 3/4 & -2 & 2 \end{pmatrix} \cdot \begin{pmatrix} J_1 \\ J_2 \\ J_3 \end{pmatrix}. \quad (3)$$

Here,  $S_B = S_1 + S_2 + S_3$ ,  $S_A = S_4 + S_5$ ,  $S = S_A + S_B$  and  $S_{B'} = S_1 + S_3$  (see the inset of figure 2).

## 2. Thermodynamic quantities

The magnetic contribution to the internal energy of the system can be derived from the following equation:

$$U_m = \frac{\sum_{\Omega} \left\{ \sum_{m_s} (-E_{\Omega}^{(0)} + m_s \bar{x} k_B T) e^{\bar{x} m_s} \right\} e^{-E_{\Omega}^{(0)}/k_B T}}{\sum_{\Omega} \left\{ \sum_{m_s} e^{\bar{x} m_s} \right\} e^{-E_{\Omega}^{(0)}/k_B T}}, \quad (4)$$

where

$$\bar{x} = \frac{g \mu_B H}{k_B T}. \quad (5)$$

The magnetic contribution to the specific heat and entropy can be derived from equation (4):

$$C_m = \frac{\partial U_m}{\partial T} \quad (6)$$

$$S_m = k_B \ln(Z_m) + \frac{U_m}{T}, \quad (7)$$

where  $Z_m$  means the magnetic contribution to the partition function and is given by the denominator of equation (4). All of these quantities will be evaluated numerically and the results discussed in the next section.

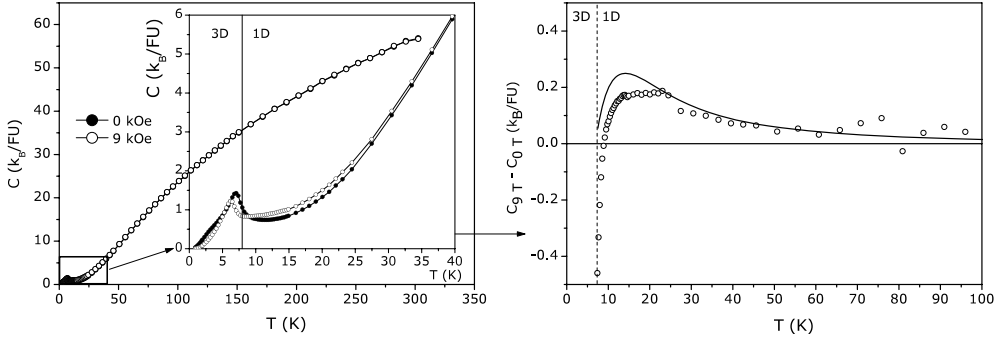


**Figure 3.** Left: experimental specific heat under 90 kOe and zero field. The inset is a detail of the low temperature regime, where a 3D phase arises below 8 K [20]. Right: difference between specific heat data, with (90 kOe) and without applied magnetic field. The full line was evaluated from equations (6) and (4) and is not a fit to the data, i.e. it was evaluated using the set  $\{J_1 = -236.20, J_2 = -8.11, J_3 = 39.89\}$  K, obtained from the analysis of the magnetic susceptibility [20].

### 3. Discussion

#### 3.1. Experimental validation of the model

In our previous work [20], we have applied this model to understand the magnetic properties of  $\text{Na}_2\text{Cu}_5\text{Si}_4\text{O}_{14}$  homometallic compound. That model returns the following exchange parameters:  $\{J_1 = -236.20, J_2 = -8.11, J_3 = 39.89\}$  K. With these values we obtained the theoretical specific heat curve, shown in figure 3. The left panel shows the experimentally observed specific heat for the  $\text{Na}_2\text{Cu}_5\text{Si}_4\text{O}_{14}$  compound, under zero and 90 kOe of applied field (measured in a PPMS Quantum Design device). Note in the inset a local peak, related to the 3D and 1D phases [20]. This transition is in fact the low temperature limit that is accessible to compare with our model. The right panel presents the difference between those two curves of specific heat ( $C_m(H=0) - C_m(H=90 \text{ kOe})$ ), and the corresponding theoretical result (from equations (4) and (6) and using those values of  $\{J_1, J_2, J_3\}$  mentioned above). It is important to emphasize the quite good agreement between experimental and theoretical results, obtained from the direct application of the model and not from a fit to the data.

Extending this analysis, figure 4 presents the magnetic contribution to the specific heat (obtained from equations (4) and (6)), as a function of temperature (top left panel), for zero and 90 kOe; and also as a function of high magnetic field (top right panel), for 10 K. This last panel is a hypothetical case, with experimentally inaccessible values of magnetic field, and shows anomalies that would be observed in this compound (if those values of magnetic field were to be reached).

Panels bottom left and bottom right present, respectively, entropy and internal energy as a function of temperature and zero magnetic field, with the corresponding limits, for  $T \rightarrow 0$  and  $\infty$  (see the appendix).

#### 3.2. General aspects of the model

It is interesting to use this simple model to look in detail at some of the most relevant features that this system would present, even beyond experimentally accessible ranges. Figure 5 presents specific heat as a function of temperature for several sets  $\{J_1, J_2, J_3\}$ . Special attention should be given to both curves numbered 3 (coincidentally the same basic structure—

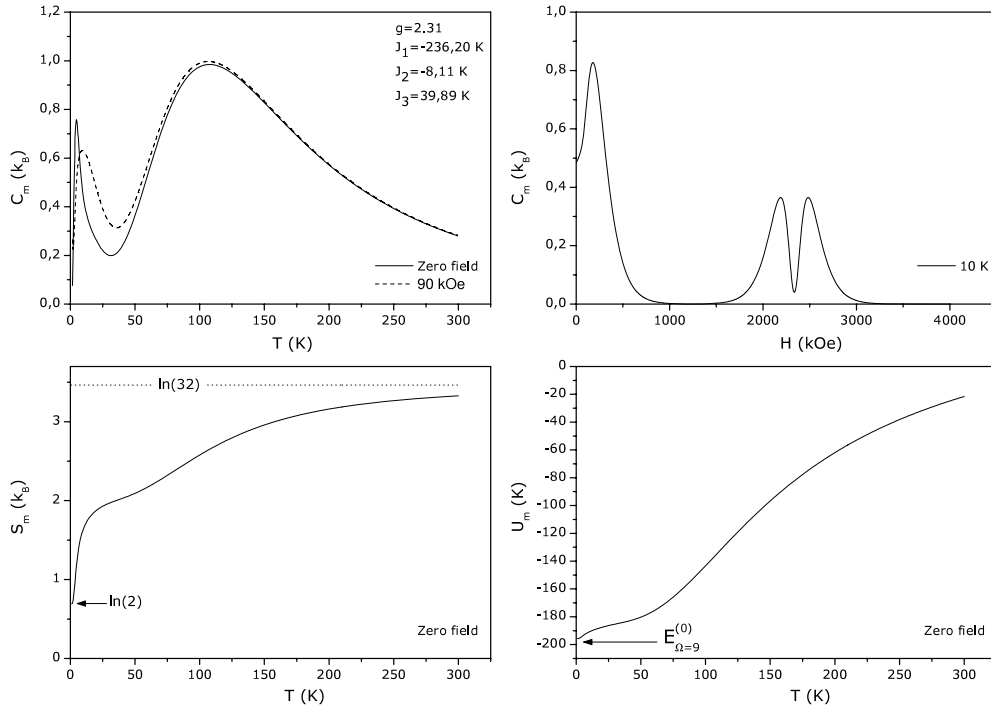


**Figure 4.** Prediction of  $C_m$  (top panels), magnetic entropy  $S_m$  (bottom left panel) and internal energy  $U_m$  (bottom right panel), as a function of temperature, for  $\{J_1 = -236.20, J_2 = -8.11, J_3 = 39.89\}$  K; values obtained in [20] for this sample  $\text{Na}_2\text{Cu}_5\text{Si}_4\text{O}_{14}$ . See the appendix for verifying the high and low temperature limits.

ferrimagnetic—as was observed for the compound presented here), where a double peak is present. Figure 6 presents the magnetic specific heat as a function of temperature for the same combination of parameters as were used for the curves numbered 3, for several values of magnetic field (zero, 5 and 10 kOe). Note that the double peak observed for high and low values of the magnetic field (zero and 10 kOe) disappears for the intermediate value (5 kOe). This feature has also been reported by Efremov and co-workers [22], for single-dimer molecules under strong magnetic field, and it is related to magnetic field induced ground state crossover, as will be discussed below.

Figure 7, top, presents the magnetic specific heat as a function of magnetic field for several temperatures. Here, those anomalies found as a function of temperature (figure 6) are reproduced, however, as a function of magnetic field. For  $T = 0.02$  K we found two peaks symmetrically centered at critical fields  $H_{c1}$  and  $H_{c2}$ . It should be noticed that an increase in temperature broadens those peaks. This feature has also been reported by Efremov *et al* [22] The bottom panel of figure 7 presents the Zeeman splitting of some quantum energy levels, highlighting the different ground states accessed by changing the magnetic field. Thus,  $H_{c1}$  corresponds to the magnetic field responsible for the first crossing of the quantum levels, changing therefore the ground state. In other words, the ground state changes from  $9 : |1/2, 1, 1/2, 1, m_s = 1/2\rangle$  to  $3 : |3/2, 1, 1/2, 1, m_s = 3/2\rangle$ , at  $H_{c1}$ . A further increasing of the magnetic field changes the ground state again, from  $3 : |3/2, 1, 1/2, 1, m_s = 3/2\rangle$  to  $1 : |5/2, 1, 3/2, 1, m_s = 5/2\rangle$ , at  $H_{c2}$ . The middle panels clarify those crossings of the quantum levels (ground states); we have plotted probability of occupancy as a function of

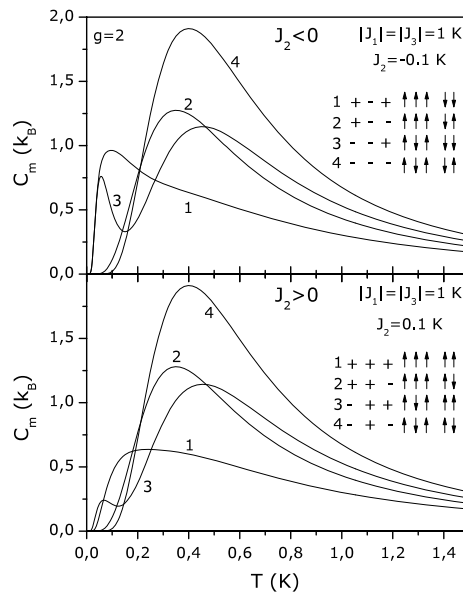


**Figure 5.** Zero-field magnetic contribution to the specific heat as a function of temperature, for several sets  $\{J_1, J_2, J_3\}$ . Note the double peak for both curves numbered 3 (top and bottom panels).

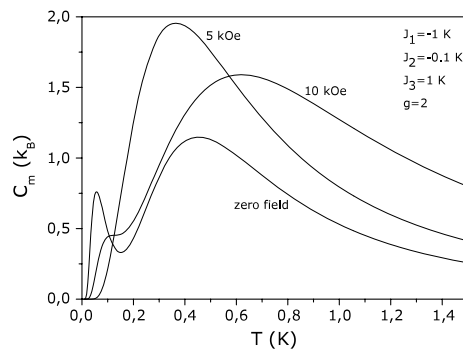


**Figure 6.** Magnetic specific heat as a function of temperature, for some values of applied magnetic field. In this case,  $J_1 = -1$  K,  $J_2 = -0.1$  K and  $J_3 = 1$  K. Note that the double peak disappears for intermediate values of magnetic field.

magnetic field, for several values of temperature. Note also the crossing of this quantity at  $H_{c1}$  and  $H_{c2}$ . It is interesting to note that close to the fields  $H_{c1}$  and  $H_{c2}$ , only the lowest two levels are relevant for sufficiently low temperatures. This yields a reduction to a two-level system which naturally explains the symmetric double-peak structure in the specific heat around those critical fields (see figure 7, top).

#### 4. Summary

In the present work we developed a model for understanding the specific heat properties of a homometallic ferrimagnetic compound  $\text{Na}_2\text{Cu}_5\text{Si}_4\text{O}_{14}$ : a low dimensional magnetic system



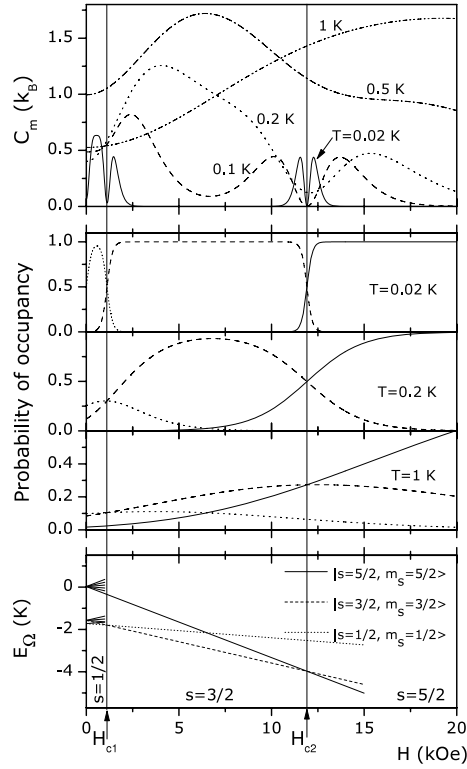


**Figure 7.** Top panel: magnetic specific heat as a function of magnetic field, for several values of temperature and  $\{J_1 = -1, J_2 = -0.1, J_3 = 1\}$  K. Middle panels: probability of occupancy of the levels  $|5/2, 1, 3/2, 1, m_s = 5/2\rangle$ ,  $|3/2, 1, 1/2, 1, m_s = 3/2\rangle$  and  $|1/2, 1, 1/2, 1, m_s = 1/2\rangle$ . Bottom panel: crossing of those quantum levels, responsible for that behavior in  $C_m(H)$ ; top panel. For the sake of clarity, we hid the other quantum levels.

with Cu dimers and trimers in a zigzag chain. We obtained excellent agreement between our model and the experimental data for the specific heat; and further analysis could predict anomalous behavior due to the crossing of energy levels.

### Acknowledgments

A M dos Santos wishes to acknowledge FCT grant BPD/14984/2004. In addition, this work was also supported by project POCT/CTM/58863/04 sponsored by FCT and FEDER, RFBR grants 06-02-16088, 07-02-00350, 07-02-91201, ISTC grant 3501 and DFG grant 486 RUS 113/864/0-1.

### Appendix. High and low temperature limits of some thermodynamic quantities

From equation (4) we can proceed to the high and low temperature limits, for  $H = 0$ :

$$U_m = -\frac{3}{8} [J_1 + 2J_3] \quad (\text{A.1})$$

$$U_m = -E_{\Omega_{GS}}^{(0)} \quad (\text{A.2})$$

respectively, where GS means ground state. For this last limit ( $T \rightarrow 0$ ), the internal energy tends to the energy of the zero-field ground state, as expected.

Since the internal energy tends to a constant value, the specific heat tends to zero in both limits (low and high temperature).

For  $H = 0$  and the  $T \rightarrow \infty$  limit,  $Z \rightarrow \sum_{\Omega} \sum_{m_s} = 32$ . The internal energy  $U_m$  tends to a constant in this limit; therefore  $S \rightarrow k_B \ln(32)$ . On the other hand, for  $H = 0$  and the  $T \rightarrow 0$  limit,  $S \rightarrow k_B \ln(\tilde{\Omega})$ , where  $\tilde{\Omega}$  is the number of accessible states of the configuration  $\Omega_{GS}$ , i.e.,  $\tilde{\Omega} = 2s + 1$ . For instance, for  $\Omega = 9 : |1/2, 1, 1/2, 1\rangle$ ,  $\tilde{\Omega} = 2$  and therefore  $S = k_B \ln(2)$ .

All of these limits are shown in figure 4.

## References

- [1] Moreira dos Santos A, Amaral V S, Brandao P, Paz F A A, Rocha J, Ferreira L P, Godinho M, Volkova O and Vasiliev A 2005 *Phys. Rev. B* **72** 092403
- [2] Feyerherm R, Mathoniere C and Kahn O 2001 *J. Phys.: Condens. Matter* **13** 2639
- [3] Coronada E, Drillon M, Nugteren P R, Dejongh L J and Beltran D 1988 *J. Am. Chem. Soc.* **110** 3907
- [4] Coronada E, Drillon M, Nugteren P R, Dejongh L J, Beltran D and Georges R 1989 *J. Am. Chem. Soc.* **111** 3874
- [5] Johnston D C, Johnson J W, Goshorn D P and Jacobson A J 1987 *Phys. Rev. B* **35** 219
- [6] Taft K L, Delfs C D, Papaefthymiou G C, Foner S, Gatteschi D and Lippard S J 1994 *J. Am. Chem. Soc.* **116** 823
- [7] Darriet J and Regnault L P 1993 *Solid State Commun.* **86** 409
- [8] DiTusa J F, Cheong S W, Broholm C, Aeppli G, Rupp L W and Batlogg B 1994 *Physica B* **181** 194
- [9] DiTusa J F, Cheong S W, Park J H, Aeppli G, Broholm G and Chen C T 1994 *Phys. Rev. Lett.* **73** 1857
- [10] Hase M, Terasaki I and Uchinokura K 1993 *Phys. Rev. Lett.* **70** 3651
- [11] Isobe M, Ueda Y, Vasiliev A N, Voloshok T N and Ignatchik O L 2003 *J. Magn. Magn. Mater.* **258** 125
- [12] Zink B L, Janod E, Allen K and Hellman F 1999 *Phys. Rev. Lett.* **83** 2266
- [13] Hagiwara M, Katori H A, Schollwock U and Mikeska H J 2000 *Phys. Rev. B* **62** 1051
- [14] Vasiliev A N, Ignatchik O L, Isobe M and Ueda Y 2004 *Phys. Rev. B* **70** 132415
- [15] Yamamoto S and Fukui T 1998 *Phys. Rev. B* **57** R14008
- [16] Nakanishi T and Yamamoto S 2002 *Phys. Rev. B* **65** 214418
- [17] Fukushima N, Honecker A, Wessel S, Grossjohanna S and Brenig W 2006 *Physica B* **359** 1409
- [18] Fukushima N, Honecker A, Wessel S and Brenig W 2004 *Phys. Rev. B* **69** 174430
- [19] Belik A A, Matsuo A, Azuma M, Kindo K and Takano M 2005 *J. Solid State Chem.* **178** 709
- [20] Reis M S, Moreira dos Santos A, Amaral V S, Brandão P and Rocha J 2006 *Phys. Rev. B* **73** 214415
- [21] Moreira dos Santos A, Brandao P, Fitch A, Reis M S, Amaral V S and Rocha J 2007 *J. Solid State Chem.* **180** 15
- [22] Efremov D V and Klemm R A 2002 *Phys. Rev. B* **66** 174427